Comparison of atherosclerotic inflammation and calcification in subjects with end stage renal disease (ESRD) on hemodialysis to normal controls utilizing ^{18}F-FDG PET/CT

Gonca G. Bural[1] MD,
Drew A. Torigian[2] MD, MA, FSAR, FACR,
Melih Sözmen[3] MD,
Mohamed Houseni[4] MD,
Abass Alavi[2] MD, PhD, DSc

1. Professor of Nuclear Medicine, Akdeniz University School of Medicine, Antalya, Turkey
2. Professor of Radiology Department of Radiology, Hospital of the University of Pennsylvania, Philadelphia, PA, USA
3. Associate Professor of Public Health, Department of Public Health, İzmir Katip Çelebi University, Atatürk Research and Training Hospital, İzmir, Turkey
4. Associate Professor of Radiology, Department of Radiology, National Liver Institute, Menoufia University, Egypt

Keywords: End stage renal disease - Hemodialysis - Atherosclerosis - Inflammation - Calcification

Corresponding author:
Abass Alavi, Professor of Radiology, MD, PhD, DSc
Hospital of the University of Pennsylvania
Tel: 215 662 3069,
Fax: 215 349 5843
abass.alavi@uphs.upenn.edu

Received:
2 September 2018
Accepted:
20 September 2018

Abstract

Objective: Subjects with end stage renal disease (ESRD) are exposed to increased morbidity and mortality due to cardiovascular events. The primary underlying mechanism has been suggested as accelerated atherosclerosis in these patients. Our aim was to compare the atherosclerotic inflammation and calcification in subjects with ESRD on hemodialysis to that in normal controls utilizing fluorine-18-2-fluoro-2-deoxy-D-glucose positron emission tomography/computed tomography (^{18}F-FDG PET/CT). **Subjects and Methods:** Forthy two subjects who underwent ^{18}F-FDG PET/CT imaging were retrospectively studied. Twenty one were subjects with ESRD on hemodialysis (67±11 years old; 14 male, 7 female) and 21 were age- and gender-matched controls. Average standardized uptake value maximum (SUVmax) and SUVmean for 4 segments of the aorta (ascending, arch, descending, abdominal) and for the common iliac arteries and common femoral arteries were measured. Standardized uptake value maximum and SUVmean for right atrial blood pool werealso measured as the background. Average SUVmax, average SUVmean, average SUVmax/background ratio, and average SUVmean/background ratiowere compared between subject groupsfor all segments. Presence or absence of macroscopic calcification on CT images for each arterial segment based on visual qualitative assessment was also noted and compared. For statistical analysis, two-sided t-test was used for continuous variables, and chi-square test was used for categorical variables. We considered a P value of <0.05 as statistically significant. **Results:** Average SUVmax and SUVmean were statistically significantly greater in subjects with ESRD than in controls in all arterial segments. Average SUVmax/background ratios were statistically significantly greater in subjects with ESRD compared to normal controls in all arterial segments except for the left femoral artery. Average SUVmean/background ratios were statistically significantly greater in subjects with ESRD compared to normal controls in all arterial segments except for the right and left femoral arteries. Presence of calcification on CT was more frequently encountered in all arterial segments in subjects with ESRD, andwas statistically significantly greater for the aortic arch, descending aorta, and right and left femoral arteries. **Conclusion:** SUV measurements representing the atherosclerotic inflammatory changes and macroscopic atherosclerotic calcifications appear to be accelerated in subjects with ESRD on hemodialysis compared to normal controls. Fluorine-18 FDG PET/CT is a valuable diagnostic tool for verifying and quantifying accelerated atherosclerosis secondary to ESRD.

Hell J Nucl Med 2018; 21(3): 169-174 *Epub ahead of print: 10 November 2018* *Published online: 5 December 2018*

Introduction

Patients with chronic kidney disease (CKD) generally experience progressive loss of kidney function resulting inendstage renal disease (ESRD). At every age, patients with ESRD on dialysis have significantly increased mortality when compared with non-dialysis patients and individuals without kidney disease. The most common cause of death overall in the dialysis population is cardiovascular disease (CVD); cardiovascular mortality is 10-20 times higher in dialysis patients than in the general population [1]. Recent studies suggest that CKD itself may be an independent risk factor for CVD [2]. Cardiovascular pathology in patients with renal failure is complex, but accelerated atherosclerosis has repeatedly been discussed as one major cause [3].

Accelerated inflammation and calcification in atherosclerosis in renal failure have already been confirmed inan animal model: Atherosclerotic lesions in the thoracic aorta were significantly larger, and the relative proportion of the calcified areas was also increased in the aortic root in uremic mice than in non-uremic controls [4]. Fluorine-18-2-fluoro-2-deoxy-D-glucose positron emission tomography (^{18}F-FDG PET) imaging has the potential to confirm these accelerated procesesses non-invasively in humans.

Fluorine-18-FDG PET/computed tomography (CT) imaging has the potential not only fordetection but also for quantification of atherosclerotic inflammatory disease. Quanti-

fication of FDG uptake is feasible using standardized uptake value (SUV) measurements [5]. Using SUV, it is also possible to determine the severity of the inflammation in atherosclerotic plaques [6]. Detection of macroscopic arterial atherosclerotic calcification is also feasible via the CT portion of PET/CT [7, 8].

Our aim was to compare the atherosclerotic inflammation and calcification in subjects with ESRD on hemodialysis to that in normal controls utilizing ^{18}F-FDG PET/CT.

Subjects and Methods

Subject sample

This retrospective study was performed after ethical committee approval was obtained from our institute. Clinical and imaging data of subjects who had undergone ^{18}F-FDG PET/CT imaging between October 2014 and December 2017 were reviewed. A total of 42 subjects were included. In the first group, 21 subjects were ESRD patients on hemodialysis (14 male and 7 female). In the other group, 21 were age-and gender-matched controls (14 male and 7 female) who had no history of ESRD or other known cardiovascular risk factors according to available clinical and laboratory data. The mean age and standard deviation (SD) for subjects in the first group with insulin-dependent diabetes mellitus (IDDM) and ESRD was 67±11 years old, and the mean age and SD for subjects in the control group was 67±11 years old (P=ns) (Table 1). Both subject groups included subjects with several different cancers referred for initial staging, restaging, or treatment response assessment.

	ESRD on hemodialysis	Controls	P
Mean age±SD years	67±11	67±11	ns
Male/Female	14/7(21)	14/7 (21)	ns
Mean blood glucose at the time of injeciton (mg/dL)	108±29	99±18	ns

Exclusion criteria for both groups included the presence of non-arterial ^{18}F-FDG uptake that interfered with arterial wall ^{18}F-FDG uptake measurement in any of the arterial segments, and the presence of extensive pathological ^{18}F-FDG uptake that overlapped with any of the arterial sites assessed in this study.

Image acquisition

Positron emission tomography/CT scans were acquired after patients had fasted for at least 4 hours and had blood glucose levels of less than 200mg/dL. There was no statistical significant difference in the mean blood glucose levels for the two groups (Table 1).

Image acquisition occurred 1 hour after injection of 3,7 MBq/kg of ^{18}F-FDG using a General Electric Discovery 710 PET/CT scanner (GE Medical Systems, Waukesha, WI, USA). The low-dose CT image acquisition was performed without injection of iodinated contrast material, followed by PET image acquisition using 3 minutes per bed position, extending from the skull vertex to the proximal thighs.

Image analysis

Image analysis was performed on a dedicated workstation (ADW 4.6, GE Medical Systems, Waukesha, WI, USA).

Averages of the maximum standardized uptake value (SUVmax) and mean standardized uptake value (SUVmean) for four segments of the aorta (ascending aorta, aortic arch, descending aorta, abdominal aorta), for the right and left common iliac arteries, and for the right and left common femoral arteries were measured and compared between both groups using transverse PET images of ^{18}F-FDG PET/ CT.

Fusion PET/CT images were used to confirm that the uptake was indeed within the arterial wall (Figure 1). For each arterial segment, ^{18}F-FDG uptake in the wall was first evaluated visually. The areas with the highest ^{18}F-FDG uptake on transverse ^{18}F-FDG PET images were chosen for that particular segment. A small region of interest (ROI) was placed over each highest uptake area within the arterial wall. For each segment, we recorded the highest SUVmax and SUVmean among all measurements. SUV measurements for ascending, arch, descending, and abdominal aorta, right and left common iliac arteries, and right and left common femoral arterial segments were measured in both groups. SUVmax and SUVmean for right atrial blood pool were also measured as the background.

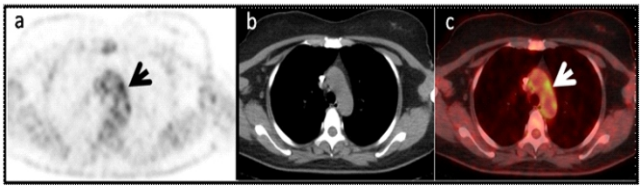

Figure 1. A 48 years old woman with ESRD on hemodialysis who underwent ^{18}F-FDG PET/CT imaging. Positron emission tomography image and fusion PET/CT image (a, c) show increased ^{18}F-FDG uptake (arrows) in walls of aortic arch due to atherosclerotic inflammation. Standardized uptake maximum value and SUVmean were 3.8 and 3.3 for aortic arch, respectively. Macroscopic atherosclerotic calcification was not detected on CT image (b) in the aortic arch.

For the detection of macroscopic atherosclerotic calcification, the transverselow-dose CT images for each of the 8 above-mentioned arterial segments in all subjects were reviewed. The presence or absence of any visible calcification within each arterial segment in both groups was recorded (Figures 2 and 3).

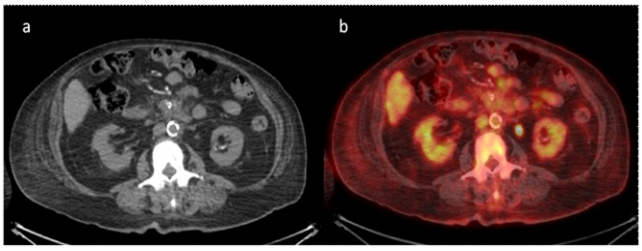

Figure 2. A 68 years old woman with ESRD on hemodialysis who underwent ^{18}F-FDG PET/CT imaging. Computed tomography image and fusion PET/CT image (a, b) show high attenuation extensive circumferential macroscopic atherosclerotic calcification in the abdominal aortic wall. Standardized uptake maximum value and SUVmean were 3.8 and 3.6 for abdominal aorta, respectively, measured from a non-calcified region.

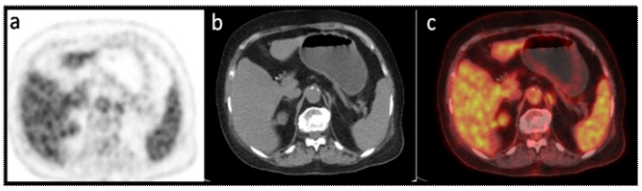

Figure 3. A 83 years old woman with ESRD on hemodialysis who underwent ^{18}F-FDG PET/CT imaging. Positron emission tomography image and fusion PET/CT image (a, c) show increased FDG uptake in walls of the abdominal aorta due to atherosclerotic inflammation. Standardized uptake maximum value and SUVmean were 2.6 and 2.5, respectively. Two small foci of high attenuation macroscopic atherosclerotic calcification weredetected on the low-dose CT image (b) at the same level.

Statistical analysis

For statistical analysis, two-sided t-test was used for continuous variables, and chi-square test was used for categorical variables. We considered a P value of <0.05 as statistically significant. Data are presented as mean and SD for continuous variables, and as numbers and percentages for categorical variables.

Results

Average SUVmax and SUVmean were statistically significantly greater in subjects with ESRD than in controls in all arterial segments (Table 2). Average SUVmax/background ratios were statistically significantly greater in subjects with ESRD compared to normal controls in all arterial segments except for the left femoral artery (Table 2). Average SUVmean/background ratios were statistically significantly greater in subjects with ESRD compared to normal controls in all arterial segments except for the right and left femoral arteries (Table 2). Presence of calcification on CT was more frequently encountered in all arterial segments in subjects with ESRD, but was statistically significantly greater for the aortic arch, descending aorta, and right and left femoral arteries (Table 3).

Discussion

Table 2. *Average SUVmax and SUVmean in subjects with ESRD and in controls*

		ESRD	Control	P value
Asc. Aorta	SUVmax	2,95	2,30	0.003*
	SUVmax/B	1,33	1,06	0.003*
	SUVmean	2,74	2,00	<0.001*
	SUVmean/B	1,38	1,10	0.002*
Arch of Aorta	SUVmax	2,92	2,24	<0.001*
	SUVmax/B	1,31	1,03	<0.001*
	SUVmean	2,59	1,94	<0.001*
	SUVmean/B	1,29	1,08	0.002*
D. Th. Aorta	SUVmax	2,93	2,35	0.014*
	SUVmax/B	1,32	1,06	<0.001*
	SUVmean	2,69	2,08	0.008*
	SUVmean/B	1,34	1,13	0.004*
Abdominal Aorta	SUVmax	3,05	2,59	0.01*
	SUVmax/B	1,37	1,17	0.005*
	SUVmean	2,79	2,24	0.004*
	SUVmean/B	1,39	1,22	0.02*
Right Iliac	SUVmax	2,61	2,23	0.04*
	SUVmax/B	1,17	1,00	0.006*
	SUVmean	2,40	2,01	0.02*
	SUVmean/B	1,19	1,10	0,01*
Left Iliac	SUVmax	2,48	2,06	0.007*
	SUVmax/B	1,12	0,94	0.01*
	SUVmean	2,24	1,80	0.001*
	SUVmean/B	1,13	0,99	0.04*
RT. Femoral	SUVmax	2,27	1,96	0.02*
	SUVmax/B	1,02	0,90	0.05*
	SUVmean	2,07	1,72	0.03*
	SUVmean/B	1,02	0,97	0,4
	SUVmean	2,03	1,85	

(continued)

LT. Femoral				
	SUVmax/B	0,98	0,87	0,09
	SUVmean/B	0,95	0,89	0,3
Back-	SUVmax	2,26	2,25	
	SUVmean	2,03	1,85	

Table 3. *Macroscopic calcification in subjects with ESRD and Control*

	ESRD	Control	P value
Ascending aorta	7	2	0,13
Arch of aorta	18	9	0.01*
Descending thoracic aorta	18	10	0.02*
Abdominal aorta	19	18	1
Right iliac	19	13	0.07
Left iliac	19	13	0.07
Right femoral	19	10	0.007*
Left femoral	19	11	0.01*

The increased frequency of cardiovascular disease observed in ESRD patients on hemodialysis patients is secondary to the combination of many classical risk factors (e.g., age, smoking, diabetes mellitus, hypertension, and hyperlipidemia). Two additional unique risk factor for these patients include uremia-related inflammation and endothelial dysfunction [9, 10]. Endothelial cell damage or injury is invariably associated with arterial atherosclerosis and may be responsible for accelerated atherosclerosis in patients with chronic renal failure [11, 12]. Vascular calcification is a well-known complication of CKD and one of the main predictors for increased cardiovascular morbidity and mortality in these patients [13]. Uremia is also reported to promote vascular calcification. Accelerated calcifying atherosclerotic lesions are also more common subjects with ESRD on hemodialysis [3].

Fluorine-18-FDG PET/CT has great potential for evaluating inflammatory conditions including atherosclerosis [14]. Inrecent years, ^{18}F-FDG PET/CT imaging has been validated as a valuablediagnostic tool for evaluating atherosclerotic inflammation [15-17]. The data showed that accurate and reproducible measurement of the inflammatory activity of atherosclerotic plaques in large and medium-sized arteries is feasible using ^{18}F-FDG PET/CT [18-24]. Inflammatory cells, predominantly the macrophages, are responsible for the increased ^{18}F-FDG uptake in atherosclerotic plaques [25].

In the current study, our data show evidence obtained from ^{18}F-FDG PET/CT that the atherosclerotic process in subjects with ESRD on hemodialysisis accelerated compared to age- and gender-matched controls.

In particular, we observed that all of the average SUV measurements were significantly greater in subjects with ESRD on hemodialysis in all arterial segments ($P<0.05$). After background correction, average SUVmax/background ratios were statistically significantly greater in subjects with ESRD compared to normal controls in all arterial segments except for the left femoral artery, and average SUVmean/background ratios were statistically significantly greater in subjects with ESRD compared to normal controls in all arterial segments except for the femoral arteries. The data show that the inflammatory component of atherosclerosis measured on ^{18}F-FDG PET/CT is more severe in subjects with ESRD on hemodialysis than in controls for the aortic segments and iliac arteries.

For the femoral arteries, SUVmax and SUVmean measurements were greater in ESRD patients than in controls. However, after background correction, only the SUVmax/background ratios were statistically significantly greater in the right femoral artery. We used the right atrial blood pool SUVmax and SUV mean as background. This could have been a confounding factor for ESRD subjects, as background blood pool uptake maybe elevated in these patients due to decreased renal excretion, potentially leading to underestimation of the severity of inflammation from atherosclerosis, particularly in the femoral arteries which are the smallest in size. There is supporting data in the literature for this above explanation, as Derlin et al. (2011) had reported that additional correction by division with blood pool SUV might lead to an over-correction, concluding that there is no reason to prefer this approach over SUVmax for the quantification of radiotracer uptake [26].

One other confounding factor could be the partial volume effect, which also has the potential for underestimation of metabolic activity. This would be expected to affect the femoral arteries the most, given they have the smallest size among small arterial segments that were assessed.

Calcification is also a delayed component of atherosclerotic process. Macroscopic atherosclerotic calcification on low-dose CT was more frequently encountered in all segments with ESRD compared to controls, although with statistical significance only for the aortic arch, ($P=0.01$), descending thoracic aorta ($P=0.02$), and right and left femoral arteries ($P=0.007$ and 0.01, respectively).

In the abdominal aorta, the number of segments with macroscopic calcification was similar in subjects with ESRD (19 subjects) compared to controls (18 subjects). The average SUVmax and SUVmean measurements were greatest in the abdominal aorta compared to all other segments in both groups, indicating that this segment was most severely affected by atherosclerotic inflammation. This may explain the reason that macroscopic calcification was frequently encountered in the abdominal aorta in both groups.

In this study, we performed qualitative visual analysis to compare the frequency of calcification between our study groups. Assessment of the calcification volumes could also have been performed for quantifying and comparing accelerated calcification due to ESRD on hemodialysis, and would likely have shown differences in the amount of macroscopic atherosclerotic calcification in all arterial segments as we qualitatively observed that the areas of calcification overall appeared to be larger in volume in ESRD patients than in controls. However, a calcium scoring program or a calcium volume measurement program was not available on our image analysis workstation, and so this was not performed. Another method which could have been used to assess atherosclerotic calcification at the molecular level is sodium ^{18}F-fluoride (Na-18F)-PET/CT imaging. However, this radiotracer is not available at our institution.

Two other limitations of this study include the small sample size and the retrospective study design. Despite these limitations, we observed statistically significant differences between the two groups of subjects.

The blood glucose levels for the two groups were slightly-greaterin subjects with ESRD on hemodialysis although without statistical significance (Table 1). There is no consensus for correcting for blood glucose levels. Some studies have found a benefit in normalizing SUV measurements by blood glucose [27-29], whereas others have found no benefit for such corrections [30-32]. A high patient serum glucose level before imaging can substantially decrease SUV measurements. If we had performed this correction, the corrected SUVs for ESRD subjects on hemodialysis would have been greater than in controls and the differences would likely have been more statistically significant, although the conclusions derived from the results would have been the same. Therefore, we decided not perform glucose correction of SUV measurements in this study.

In conclusion, our data suggest that ^{18}F-FDG uptake representing atherosclerotic inflammatory changes and macroscopic atherosclerotic calcifications appear to be accelerated in subjects with ESRD patients on hemodialysis compared to normal controls. Fluorine-18-FDG PET/CT is a powerful non-invasive diagnostic tool that can detect and quantify the accelerated inflammatory atherosclerotic process in patients with ESRD on hemodialysis.

Bibliography

1. Wald R, Yan AT, Perl J et al. Regression of left ventricular mass following conversion from conventional hemodialysis to thrice weekly in-centre nocturnal hemodialysis. *BMC Nephrol* 2012; 13: 3.
2. Balla S, Nusair MB, Alpert MA. Risk factors for atherosclerosis in patients with chronic kidney disease: recognition and management.*Curr Opin Pharmacol* 2013; 13: 192-9.
3. Amann K, Tyralla K, Gross ML et al. Special characteristics of atherosclerosis in chronic renal failure. *Clin Nephrol* 2003; 60 Suppl 1: S13-21.
4. Ivanovski O, Nikolov IG, Drueke BT et al. Atherosclerosis and vascular calcification in uraemia - a new experimental model. *Prilozi* 2007; 28: 11-24.
5. Pasha AK, Moghbel M, Saboury B et al. Effects of age and cardiovascular risk factors on ^{18}F-FDG PET/CT quantification of atherosclerosis in the aorta and peripheral arteries. *Hell J Nucl Med* 2015; 18(1): 5-10.
6. Bural GG, Torigian DA, Basu S et al. Atherosclerotic inflammatory activity in the aorta and its correlation with aging and gender as assessed by ^{18}F-FDG-PET. *Hell J Nucl Med* 2013; 16(3): 164-8.
7. Meirelles GS Gonen M, Strauss HW. ^{18}F-FDG uptake and calcifications in the thoracic aorta on positron emission tomography/computed tomography examinations: frequency and stability on serial scans. *J Thorac Imaging* 2011; 26: 54-62.
8. Bural GG, Torigian DA, Botvinick E et al. A pilot study of changes in ^{18}F-FDG uptake, calcification and global metabolic activity of the aorta with aging. *Hell J Nucl Med* 2009; 12(2): 123-8.
9. Bossola M, Tazza L. Wishful Thinking: The Surprisingly Sparse Evidence for a Relationship between Oxidative Stress and Cardiovascular Disease in Hemodialysis Patients. *Semin Dial* 2015; 28: 224-30.
10. Garimella PS, Hirsch AT. Peripheral artery disease and chronic kidney disease: clinical synergy to improve outcomes. *Adv Chronic Kidney Dis* 2014; 21: 460-71.
11. Malyszko J. Mechanism of endothelial dysfunction in chronic kidney disease. *Clin Chim Acta* 2010; 411(19-20): 1412-20.
12. Kanbay M, Afsar B, Gusbeth-Tatomir P et al. Arterial stiffness in dialysis patients: where are we now? *Int Urol Nephrol* 2010; 42: 741-52.
13. Ossareh S. Vascular calcification in chronic kidney disease: mechanisms and clinical implications. *Iran J Kidney Dis* 2011; 5: 285-99.
14. Bural GG, Torigian DA, Houseni M et al. Is ^{18}F-FDG PET/CT a valuable diagnostic tool for verifying accelerated atherosclerosis secondary to diabetes mellitus on insulin in the aortic segments and large arteries? *Hell J Nucl Med* 2017; 20(3): 192-7.
15. Lawal I, Sathekge M. F-18 FDG PET/CT imaging of cardiac and vascular inflammation and infection. *Br Med Bull* 2016; 120: 55-74.
16. Aboagye EO, Kraeber-Bodéré F. Highlights lecture EANM 2016: "Embracing molecular imaging and multi-modal imaging: a smart move for nuclear medicine towards personalized medicine". *Eur J Nucl Med Mol Imaging* 2017; 44: 1559-74.
17. Joseph P, Tawakol A. Imaging atherosclerosis with positron emission tomography. *Eur Heart J* 2016; 37(39): 2974-80.
18. Ogawa M. ^{18}F-FDG accumulation in atherosclerotic plaques: immunohistochemical and PET imaging study. *J Nucl Med* 2004; 45(7): 1245-50.
19. Davies JR. FDG-PET can distinguish inflamed from non-inflamed plaque in an animal model of atherosclerosis. *Int J Cardiovasc Imag* 2011; 26: 41-8.
20. Bural GG. Torigian DA, Chamroonrat W et al. FDG-PET is an effective imaging modality to detect and quantify age-related atherosclerosis in large arteries. *Eur J Nucl Med Mol Imag* 2008; 35(3): 562-59.
21. Chen W, Bural GG, Torigian DA, et al. Emerging role of FDG-PET/CT in assessing atherosclerosis in large arteries. *Eur J Nucl Med Mol Imaging* 2009; 36: 144-51.
22. Metha NN, Torigian DA, Gelfand JM et al. Quantification of atherosclerotic plaque activity and vascular inflammation using [^{18}F] fluorodeoxyglucose positron emission tomography/computed tomography (FDG-PET/CT). *J Vis Exp* 2012; e3777.
23. Huet P, Burg S, Le Guludec D et al. Variability and uncertainty of ^{18}F-FDG PET imaging protocols for assessing inflammation in atherosclerosis: suggestions for improvement. *J Nucl Med* 2015; 56: 552-9.
24. Marzola MC, Saboury B, Chondrogiannis S et al. Role of FDG PET/CT in investigating the mechanisms underlying atherosclerotic plaque formation and evolution. *Rev Esp Med Nucl Imagen Mol* 2013; 32: 246-52.
25. Basu S, Zhuang H, Torigian DA et al. Functional imaging of inflammatory disease using nuclear medicine techniques. *Semin Nucl Med* 2009; 39: 124-45.
26. Derlin T, Habermann CR, Lengyel Z et al. Feasibility of ^{11}C-acetate PET/CT for imaging offatty acid synthesis in the atherosclerotic vessel wall. *J Nucl Med* 2011; 52: 1848-54.
27. Krak NC, van der Hoeven JJM, Hoekstra OS et al. Measuring ^{18}F-FDG uptake in breast cancer during chemotherapy: comparison of analytical methods. *Eur J Nucl Med Mol Imag* 2003; 30: 674-81.
28. Avril N, Bense S, Ziegler SI et al. Breast imaging with fluorine-18-FDG PET: quantitative image analysis. *J Nucl Med* 1997; 38: 1186-91.
29. Wong CY, Thie J, Parling-Lynch KJ et al. Glucose-normalized standardized uptake value from ^{18}F-FDG PET in classifying lymphomas. *J Nucl Med* 2005; 46: 1659-63.

30. Stahl A, Ott K, Schwaiger M et al. Comparison of different SUV-based methods for monitoring cytotoxic therapy with FDG PET. *Eur J Nucl Med Mol Imag* 2004; 31: 1471-8.
31. Vriens D, de Geus-Oei L, van Laarhoven HW et al. Evaluation of different normalization procedures for the calculation of the standardized uptake value in therapy response monitoring studies. *Nucl Med Commun* 2009; 30: 550-7.
32. Sanghera B, Emmott J, Wellsted D et al. Influence of N-butylscopolamine on SUV in FDG PET of the bowel. *Ann Nucl Med* 2009; 23: 471-8.

Thomas Gainsborough 1727-1788. Portrait of a Lady in Blue. Late 1770s.